Energy & Buildings 306 (2024) 113946

Contents lists available at ScienceDirect

Energy & Buildings

journal homepage: www.elsevier.com/locate/enb

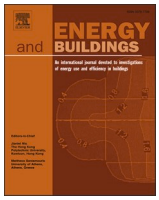

Design of three outdoor combined thermal comfort prediction models based on urban and environmental parameters

Laura Pompei [a], Fabio Nardecchia [a], Luca Gugliermetti [b,*], Federico Cinquepalmi [b]

[a] Department of Astronautic, Electric and Energy Engineering (DIAEE), Faculty of Engineering, Sapienza University of Rome, Via Eudossiana 18, Rome, Italy
[b] Department of Architecture and Design (DIAP), Faculty of Architecture, Sapienza University of Rome, Via Flaminia 359, Rome, Italy

ARTICLE INFO

Keywords:
Urban environment
Microclimate
Outdoorthermal comfort
Predictive models
CFD

ABSTRACT

The current trend of urbanization growth, take along a substantial increase in the outdoor temperatures within built environments, affecting the liveability of outdoor space, reducing the thermal comfort of citizens. Outdoor thermal comfort is usually evaluated with complex models on large scale, considering neighbourhoods, districts, or cities, without focusing on local and accurate predictions. The present study is aimed at contributing to the topic by proposing a simple yet accurate combined prediction model, able to assess the outdoor thermal comfort around a theoretical isolated building. A set of parameters, such as wind velocity, relative humidity, solar irradiation, and building height, has been used to quantify their effect urban comfort at fixed air temperature. The same parameters have been used for the development of a predictive correlation for the three outdoor thermal comfort indexes (UTCI, PET and SET). Comfort data was calculated by CFD simulations where the environmental parameters was variated in a fixed range. The main contribution to outdoor thermal comfort is provided by solar irradiation affecting the comfort indexes values up to 50%, the second is the wind velocity affecting up to 25% the thermal comfort indexes. The variation of building height is less impacting (around 15% of comfort values) as well as the relative humidity (5%). At least, three correlations have been elaborated for each outdoor thermal index. Correlation's quality has been evaluated using RMSE and percentage difference, obtaining a maximum average value of 0.71 and 1.48%, respectively.

1. Introduction

During the last decades, cities were growing quickly without an integrated plan for urban spaces management [1]. This fast growth has negatively affected the local urban climate increasing the outdoor temperature and reducing the thermal comfort of citizens. Nowadays, people spend ever more of their time outdoors for leisure and working activities regardless of the season, so they are exposed to varying thermal conditions, ranging from thermal stress up to neutral, comfortable conditions [2]. Furthermore, there is a direct relation with the reduction in the amount of energy spent on air conditioning and lighting, and the amount of time spent outdoors [3,4]. Thermal comfort affects people's physical strain and health, influencing the liveability of urban spaces [5]. Health and well-being can be seriously compromised in the case of extreme heat or cold environments [6]. As evidenced in many studies, high outdoor temperatures and humidity can be also correlated with the concentration of pollutants in the air [7–9]. Moreover, the effect of temperature and humidity alters the effectiveness of viruses, bacteria, and moulds on people's health [10,11]. Therefore, it is essential to study thermal comfort in urban areas to increase the citizen's quality of life, contributing to their well-being and to the quality of the time they spend outside. However, it is a subjective evaluation as evidenced in the ASHRAE standard [12].

Urban thermal comfort considers many key performance indicators since its assessment is affected by both qualitative and quantitative factors. Scientific literature shows more than 200 thermal comfort indexes developed during the last twenty years [13–15]. Nowadays, Universal Thermal Climate Indexes (UTCI) and Physiological Equivalent Temperatures (PET) are the most used benchmarks [2]. The PET index is based on the Munich Energy-balance Model for Individuals (MEMI) which considers all the basic thermoregulatory processes that occur in the body [15]. Instead, the UTCI uses a temperature control index for clothing developed by the International Society of Biometeorology developed using together the "Fiala thermoregulation model" and an adaptive clothing model [16,17]. Another suitable index is the Standard

* Corresponding author at: Department of Architecture and Design (DIAP), Faculty of Architecture, Sapienza University of Rome, Via Flaminia 359, 00196 Rome (RM), Italy.
E-mail address: luca.gugliermetti@uniroma1.it (L. Gugliermetti).

https://doi.org/10.1016/j.enbuild.2024.113946
Received 3 October 2023; Received in revised form 8 January 2024; Accepted 23 January 2024
Available online 26 January 2024

Nomenclature

ANN	Artificial Neural Network
ASHRAE	American Society of Heating, Refrigerating and Air-Conditioning Engineers
BK	Back façade
CFD	Computational Fluid Dynamic
DO	Discrete Ordinates
FR	Frontal façade
GMT	Greenwich Mean Time
H	Building height [m]
I	Global solar radiation [W/m^2]
LT#	Lateral façade number
MEMI	Munich Energy-balance Model for Individuals
P#	Probed point number
PET	Physiological Equivalent Temperature [°C]
PISO	Pressure-Implicit with Splitting of Operators
RANS	Reynolds-Averaged Navier-Stokes
RH	Relative Humidity [%]
RMSE	Root-Mean-Square Error
RTE	Radiative Transport Equation
S_{cr}	Heat stored in a node placed inside the body
SET	Standard Effective Temperature [°C]
S_{sk}	Heat in a node placed on the skin
T_a	Outdoor air temperature [°C]
T_c	Body temperature [°C]
T_{cl}	Clothes temperature [°C]
T_l	Local temperature [°C]
T_{mr}	Mean radiant temperature [°C]
T_{sk}	Skin temperature [°C]
U	Outdoor wind speed [m/s]
UTCI	Universal Thermal Climate Index [°C]
Δ%	Percentage error [–]

Effective Temperature (SET), which is based on an equivalence between the perceived comfort of a normal clothed person inside a virtual environment and the comfort in the actual environment with actual clothing and activity level [18]. Since SET is independent from the environment, it is suitable for most meteorological conditions [13,15]. Most of the outdoor thermal indexes use physical factors (clothing insulation, metabolic activity, skin temperature, and body composition), as pointed out [19] and employ four environmental parameters, air temperature, mean radiant temperature (T_{mr}), air velocity, and relative humidity [20]. Those environmental parameters play an essential role in the definition of the thermal comfort of citizens; therefore, their variation allows to understand their mutual and combing impacts on the microclimate [21].

How evidenced by many works on the topic, outdoor thermal comfort is a widely discussed topic around the international scientific community. The scientific review of P. Kumar and A. Sharma [22] showed a consistent global increase in the total number of studies made during the last twenty years, with most of them developed in Europe, South Korea, Japan, Bangladesh, Australia, and North America. During the 13 years between 2001 and 2014, only 49 papers were published, fewer than the 72 published in the 4 years between 2015 and 2019. This increase is directly related to the ever-increasing attention on the climate change. F. Ali-Toudert and H. Mayer, [23] developed a numerical analysis of the effects related to the aspect ratio and orientation of urban street canyons on outdoor thermal comfort. The study was developed with ENVI-met software and has a case study a summer day in Ghardaia, Algeria. Authors employed a statistical descriptive analysis and an inferential method to calculate PET value with the software RayMan. The results evidenced a low influence of all three SEM environments on the thermal sensation votes. N. Abdollahzadeh and N. Biloria [24] studied the impact of urban configuration (street orientation, aspect ratio, building topology, and surface coverage) using computational simulation models to assess outdoor thermal comfort in Sydney. Their results found that among the meteorological parameters (air temperature, wind speed, humidity, and solar radiation), wind velocity had the most significant impact on thermal comfort in coastal regions, which typically are subjected to intense airflows. However, other studies developed in zones far from the coasts evidenced the aspect ratio and street canyon orientation as the most important factors for outdoor comfort [25,26]. Another interesting study was made by R. Shah et al. [27] that developed an ANN (Artificial Neural Network) model to predict PET and UTCI in street canyons. Their study demonstrates how air temperature could be used as the only microclimatic input parameter to predict thermal comfort indexes with a surprising, good accuracy. Among the outdoor adaptive thermal comfort model, T. Xu et al. [5] developed a quantitative one that is a function of the exponentially weighted sum of the measured historical mean air temperature. The model was developed using questionaries and showed how UTCI models are more restrictive considering the actual acceptable thermal comfort range. As suggested by the literature, the need of developing a predictive and accurate model of a building for outdoor thermal comfort is a requirement to improve comfort of pedestrians [38] and to guide the future mitigation strategies for urban microclimate [39]. The study of environmental outdoor condition at local scale (single and isolated buildings) has always interested the scientific community and international literature is full examples of models and simulations on this topic [28–34]. However, as evidenced by the scientific review of Aghamolaei et al. [34], there are very few works related to thermal comfort evaluation, especially if the contribution of humidity is evaluated. Moreover, an isolated building can be intended as part of a local urban agglomerate, separated by wide courtyards and open spaces, thus acting as a link between urban and local scales for outdoor thermal studies [35–38]. Geometric parameters such as height-to-width ratios, orientations and layouts can be used to improve ventilation and pedestrians' thermal comfort. Although several studies were conducted on a larger scale such as neighbourhoods, districts, or cities, their results are often limited to a certain times and locations, limiting their overall applicability [37]. The present work is intended to fill this gap proposing a simple yet exportable methodology for thermal comfort assessment by proposing a set of predictions model able to assess the outdoor thermal comfort (PET, SET, UTCI) around an isolated building. The few physical quantities required by the model proposed (wind velocity, relative humidity, solar irradiation, and building height) allow to easily quantify which parameters affect most the comfort and permits to calculate the three outdoor thermal comfort indexes mentioned. Computational fluid dynamic simulations have been used to investigate the effects of input parameter variations and to develop the correlations database. The main outcomes of the presented works are (1) a parametric analysis of the impact of the urban and environmental parameters on outdoor thermal comfort; (2) the development of the correlations based on few parameters; (3) evaluation of the results. Section 2 describes the model setting and domain mesh applied for the CFD simulations as well as the calculation of the selected outdoor thermal indexes. Section 3 reports the main results divided into two macro-categories: firstly, highlighting the single influence of the parameters on PET, SET, and UTCI; then, describing the results of three correlations. This work is based on a previous paper where the impact of humidity on vortex creation was studied for the same building's layouts [33].

2. Methods

The methodology for the elaboration of models and their assessment is developed by a progressive approach; as first, a typical isolated building is identified in terms of dimensions (height of the building), orientation, and environmental conditions (air temperature, pressure, relative humidity, irradiation, and wind velocity) [32,33]. Secondly, a set of 13 CFD simulations were performed basing on the building data by changing a single parameter at time (height of the building, relative humidity, irradiation, and wind velocity). As third, thermal comfort indexes (PET, SET, and UTCI) were calculated on 12 points located near the building using the commercial software RayMan and UTCI. Then, the results were evaluated, and three different correlations were developed by fitting data thermal comfort data by a MATLAB custom code. At least the results and the errors has been calculated. All the steps are reported in Fig. 1.

2.1. Model setting: numerical problems, geometrical inputs, and mesh domain

Computational Fluid Dynamics (CFD) simulations have been performed using the commercial software Ansys Fluent v.14.5 (2013b). The validation of the proposed CFD model was already presented and discussed in a previous work by a comparison with experimental measurements as well as the numerical set-up and governing equations of the physics problem, and the physical reasons behind their choices [32,33]. However, the main information has been resumed to facilitate the comprehension of the presented research. The set-up of the simulations is the following: 3D double precision solver, pressure-based solver, steady-state analysis, and RANS steady equations with standard k-ε model. PISO algorithm has been used to couple the pressure–velocity. Convection and viscous terms of the governing equations have been calculated using second-order discretization and pressure interpolation schemes. As turbulent flows solver, Ansys Fluent uses RANS steady equations for the balance of both mass momentum and energy. The application of the k-ε model has been chosen because it is the most suitable turbulence model employed in CFD codes for the analysis of the phenomenon far from the interface surfaces [40]. K-ε model solves the Reynolds-Averaged Navier-Stokes (RANS) equations coupled with transport equations for the turbulent kinetic energy, k, and its dissipation rate, ε. It is important to underline that only the mean flow is calculated by this model; instead, turbulence is parameterized at all scales using appropriate laws [33,41,42]. To determine convergence, all the scaled residuals must level off and have a minimum value of 10^{-6} for momentum in x, y, z, and k.

Geometrical input has been configured following the guidelines proposed by [43] for the computational domain. In the case of outdoor studies, the maximum vertical dimension of the domain above the roof of the building should be at least 5H, where H is the building height. To correctly develop wind profiles, the same condition (at least 15H) has been defined for the distance between the inlet surface and the windward wall. Additionally, a distance of 15H has been used between the side walls of the building and the domain boundaries. As final step, the outflow surface has been positioned at 15H far from the leeward surface to allow the wake to fully develop (Fig. 2). The geometrical dimensions of the isolated buildings are the following: 5 m of with, 10 m of depth and the height is variable.

The domain has been discretized by using an orthogonal grid. To enhance the quality of the mesh has been employed a block-based hexahedral mesh since the geometry was relatively simple. Close to the solid surfaces (the ground, rooftops, and building walls), grid lines have been refined, and the space between grid lines has been gradually increased with the distance from solid surfaces using an inflation ratio of 1.15. Four grid meshes (A, B, C and D) characterized by different densities have been developed (Table 1). In each model, probes have been placed so as not to be influenced by turbulent phenomena and wind speed has been compared across the four grids [33]. Mesh A (about 2,900,000 cells) has assumed as the reference case. Table 1 shows that there is only a 2 % difference (Δ%) between Mesh A and the finest mesh (Mesh D), demonstrating the robustness of the simulation and computing time. As it was done for the paper of Nardecchia et al. [33], Mesh A has been chosen for the CFD investigation.

Moreover, a grid independence test has been performed to validate the model, and a mesh of about 2,900,000 cells has been applied to this study [33,43]. To define air vertical velocity profile at inlet, a logarithmic law function has been used with a turbulence value of 5 %. For the ground roughness coefficient, the one proposed by Launder and Spalding [44] has been chosen, following the considerations of Cebeci and Bradshaw [45]. Moreover, to avoid crossflowing, a condition of null air velocity has been applied as boundary condition at the lateral and upper sides. The environmental parameters have been set to 101.325 kPa for pressure (standard condition) and 303 K for air temperature (as reference of Ansys Fluent Database). The airflow perpendicularly impacts the building.

Considering the optical proprieties of walls and soil, their infrared and visible absorption coefficients has been respectively imposed to 0.8 and 1.0 with a purely diffusive reflection, as suggested by Bottillo et al. [46]. The Radiative Transport Equation (RTE) for a finite number of discrete solid angles using the radiative model Discrete Ordinates (DO) has been used to add the radiative contribution to the simulation. For simulating real climatic conditions and setting different radiation intensities, the Solar-Ray Tracing model in Solar Load Model has been activated inside Ansys Fluent. The coordinates used for the simulation corresponds to latitude 41° 53′ and longitude 12° 29′, the geographic

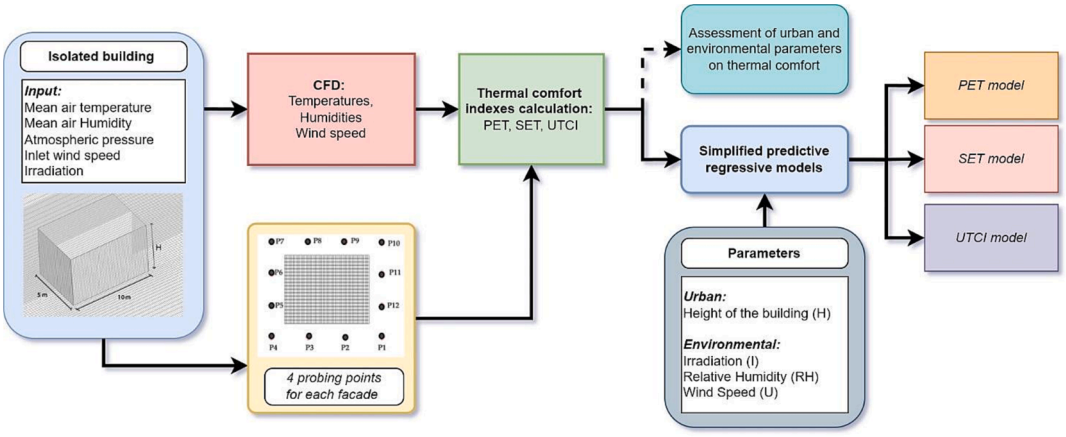

Fig. 1. Methodological flow chart.

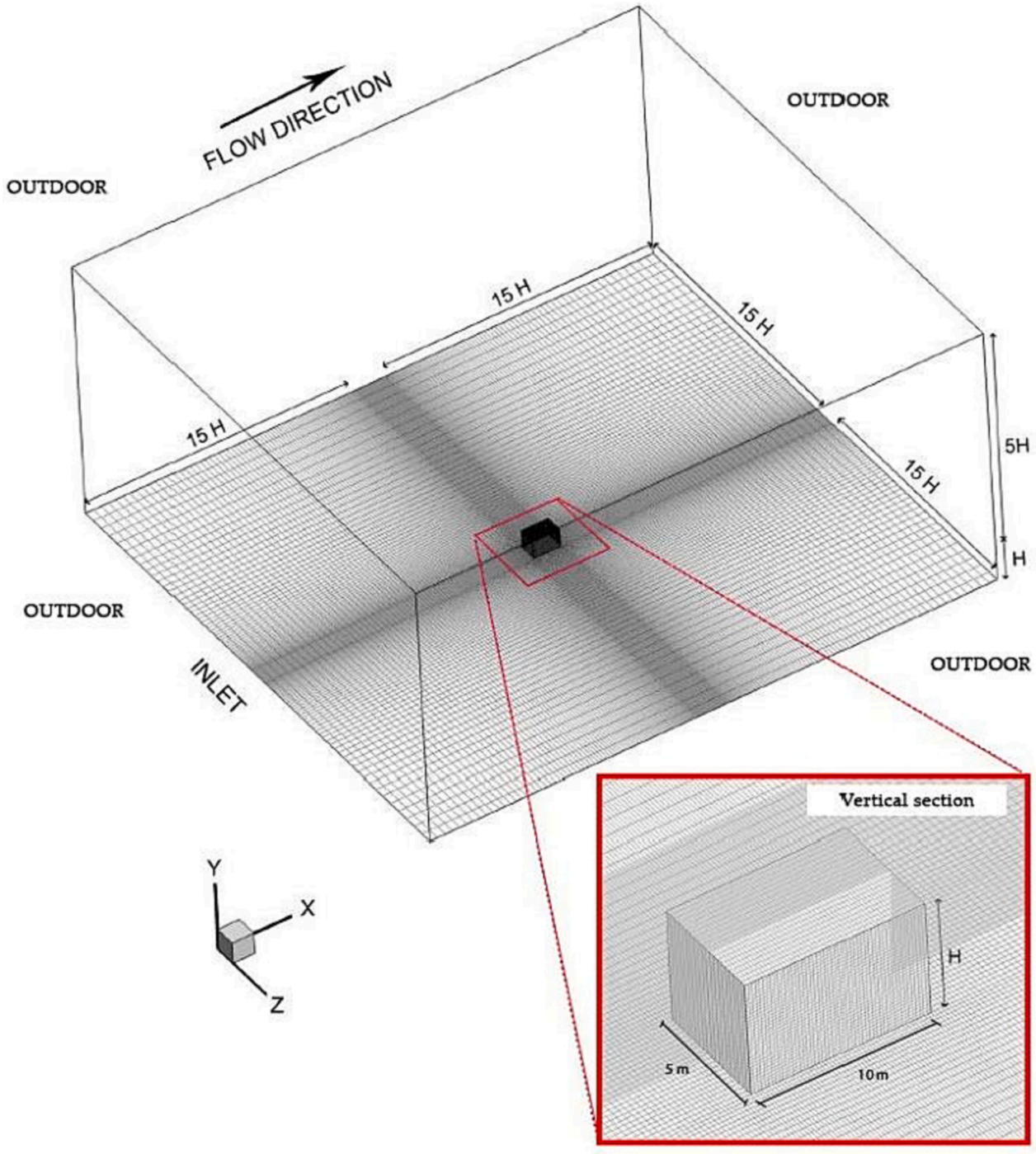

Fig. 2. Calculation domain, mesh, and geometry. In the red square is visible the detail of the simulated building [31]. (For interpretation of the references to colour in this figure legend, the reader is referred to the web version of this article.)

Table 1
Four mesh sensitivity properties and the corresponding percentage difference [33].

	Mesh A	Mesh B	Mesh C	Mesh D
Total n° of cells	2,900,000	700,000	1,300,000	6,000,000
Mesh interval size (m)	0.1	0.5	0.25	0.05
$\Delta_{\%}$	–	33	20	2

coordinates of Rome at 13.00 GMT on 21 June (solar angle at 65° above the horizontal plane).

Instead, shell conduction hypothesis has been made to simulate the heating of walls and ground, as recommended by Bottillo et al. [46]. This allows assuming a conduction exchange without the need of meshing the thickness of the walls, thus reducing the simulation's complexity. For the ground, as starting temperature has been chosen the value of 288 K, the specific heat has been imposed to 1 kJ/kgK, the thermal conductivity to 2 W/mK, and the density to 1000 kg/m^3 [32]. The building's walls have been simulated to be similar to the ground, but with a thermal conductivity of 0.15 W/mK [32]. Moreover, their

thickness has been assumed to be 0.30 m.

During the simulation process several selected steps of the solving process were controlled to avoid uncontrolled oscillations, such as velocity and temperature. As for the sensitivity analysis as convergence parameter has been used the axial scaled momentum value of 10^{-6}.

2.2. Outdoor thermal comfort indexes

Thermal comfort is essentially defined by external climatic conditions: ambient temperature, average radiant temperature, wind speed, and relative humidity. Additional elements are also involved such as the clothing worn, metabolism, activity, and individual's adaptability to the microclimate [12]. To quantify the temperature perception of the surrounding environment by individuals, several thermal comfort indexes are available, both for indoor and outdoor places [15]. Generally, the indexes are essentially divided into two broad categories. The first one, as for SET, collects the parameters evaluated as a function of a reference environment that produces the same thermal stress on the individual; the second category of indexes is based on the "vote" that a homogeneous group of people express regarding of a specific context, an example is represented by UTCI. A certain thermal sensation is assigned to the second category indexes, usually through a system of weighted surveys based on the climatic situation wherein the interviewee is located. The result is to get a point on a scale to each index value, such as the seven-point exposed in [47]. In this research, the following outdoor thermal comfort indexes have been chosen, because they are the most representative for the case in analysis [47].

- PET, Physiological Equivalent Temperature
- SET, Standard Effective Temperature [15]
- UTCI, Universal Thermal Climate Index [16,17]

Moving to the outdoor thermal indexes, both RayMan [48] and UTCI [16] software have been chosen. The first one allows us to calculate PET and SET, and the other one UTCI index. RayMan [49] software is based on the estimation and calculation of the Mean Radiant Temperature (MRT) which is required in the energy balance model. Using the software, it is possible to calculate the radiation fluxes and estimate shading and reflexes (direct and diffuse) caused by the surroundings. Those data are necessary for the sky view factor calculation, used to weight the solar irradiation within the thermal comfort models. The calculation requires a few essential information related to the urban landscape as the presence of shading elements, the characteristic of the horizon, air temperature, relative humidity, environmental pressure, and wind velocity. Instead, UTCI has been calculated with the online free calculator developed by the "International Society of Biometeorology" [16,17]. The main parameters required by the UTCI calculator are the air temperature, the mean radiant temperature, the relative humidity, the vapour pressure, and the wind velocity.

2.3. Environmental and urban variables

The modelled building has a width of 5 m, a depth of 10 m and a variable height (H). The environmental parameters used in the simulation are the following: irradiation (I), relative humidity (RH) and wind velocity (U). During the simulations, one of the parameters (U, I, H, RH) has been varied considering the other parameters at a representative fixed value. This value has been chosen because is the most probable during the season basing on historical climate data (database: Ansys Fluent). The parameters ranges are shown in Table 2. A total of 12 simulations have been performed considering the single contribution of inlet velocity, temperature, radiation, building's height and, relative humidity to thermal comfort. Cases in bold (Table 2) represents the representative case and they appear four times due to the variation of a single parameter per time.

The inlet air temperature (T_{air}) has been set to 303 K as reference from Ansys Fluent database and environmental pressure at standard conditions 101.325 kPa. As previously mentioned, the model has been placed at 41° 53′ of latitude and 12° 29′ of longitude, corresponding to the geographic coordinates of Rome at 13.00 GMT on 21 June, when the solar angle is about 65° above the horizon. The building is oriented with North in front of the FR façade.

Table 2
Characteristics of the twelve combinations. In bold the representative values of the parameter.

Case	I – direct \ diffuse (W/m^2)	H (m)	U (m/s)	Relative Humidity (%) – RH
1	1400\600	10	0.50	50
0	**1000\400**	**10**	**0.50**	**50**
2	600\200	10	0.50	50
3	200\50	10	0.50	50
4	1000\400	5	0.50	50
0	**1000\400**	**10**	**0.50**	**50**
5	1000\400	20	0.50	50
6	1000\400	30	0.50	50
7	1000\400	10	0.10	50
10	**1000\400**	**10**	**0.50**	**50**
8	1000\400	10	1	50
9	1000\400	10	2	50
0	**1000\400**	**10**	**0.50**	**50**
10	1000\400	10	0.50	60
11	1000\400	10	0.50	70
12	1000\400	10	0.50	80

The data relating to local temperature (T_l), wind speed (U), relative humidity (RH) and average radiant temperature (T_{mr}) has been collected at each point basing on the simulations. Obtaining those data from Ansys Fluent it is possible to use it for thermal comfort calculations.

As shown in Fig. 3, four points have been selected per each façade: side 1 (T_1), side 2 (LT_2), Front (FR) and Back (BK), at 1 m from the wall and 1.5 m from the ground, a height suitable for the perception of the well-being of the average individual [50]. As distance between each point has been chosen 5.67 m (on x-axis) and a height from the ground of 1.5 m (on y-axis).

Because of the different development of air turbulence in the front, side, and back of a building, it was necessary to analyse the entire area that surrounds the building. Moreover, the level of radiation that reaches the points depends on the geometry of the building facades, especially from the height and orientation.

3. Results

This section illustrates the main results coming from the simulations. The results have been reported varying a singular parameter at a time (i.e., irradiation, building height, velocity, and relative humidity), defining 16 different combinations. Detailed results of the Fluent model can be consulted in the previous paper published by the authors [33]. Then three correlations have been proposed to predict the outdoor thermal indexes (SET, PET, UTCI) with the simultaneous variation of the main parameters involved, except for the relative humidity (Section 3.5).

3.1. Irradiation effect on thermal comfort

Irradiation influences the thermal condition near a building heating exposed surfaces due to the absorption of radiative energy. In general, what is obtained by inserting a radiative model is the calculation of the energy received and emitted by each surface exposed to the sun. As shown in Fig. 4, the FR and LT2 are the facades with high values of irradiation, with $6.02{\cdot}10^2$ W/m^2 and $1.31{\cdot}10^3$ W/m^2 respectively. To give an overview of the thermal variability in each point, façade LT1 has been chosen as reference because it presents a trade-off in the four points, some are in a sunny area and others to shadowed.

Fig. 4 reports the results of PET, SET and UTCI, whit the following

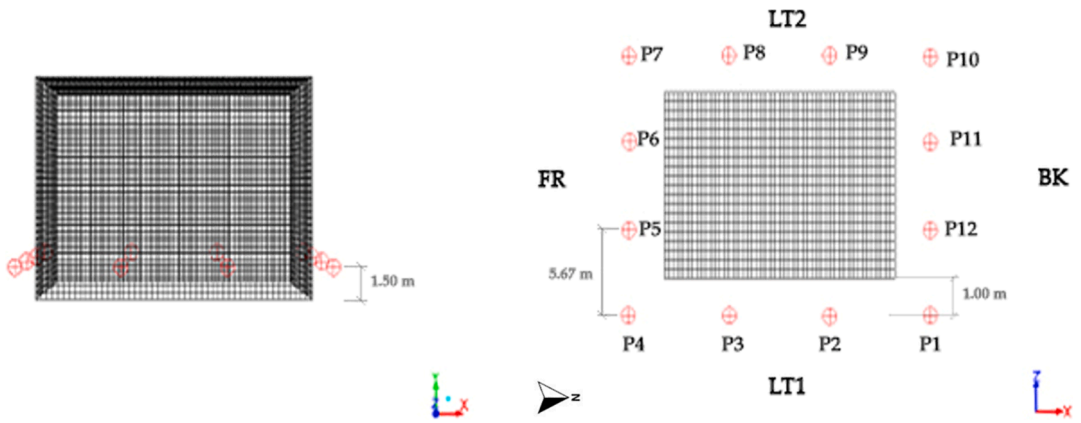

Fig. 3. Points are chosen for each façade of the isolated building. Red markers are the measurement points used for thermal comfort calculations. (For interpretation of the references to colour in this figure legend, the reader is referred to the web version of this article.)

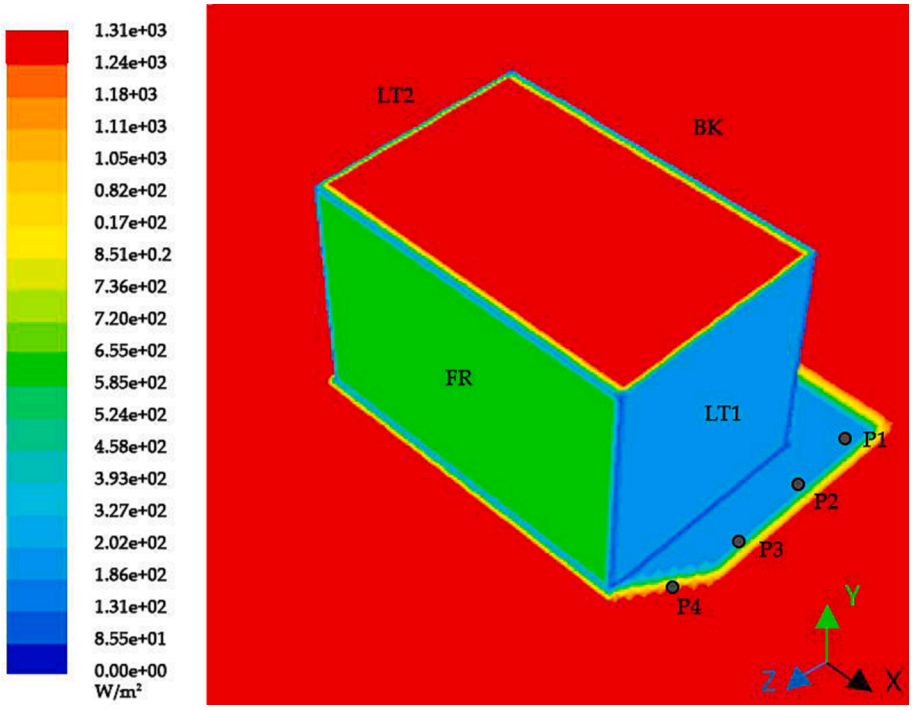

Fig. 4. Irradiation analysis on LT_1 façade.

values set, 0.5 m/s of wind velocity, 50 % RH, 10 m for building height and irradiation of 1400\600 W/m^2. PET registered the maximum percentage difference between P1 and P4, equal to 15 % since P1 obtained 59.90 °C and P2 68.90 °C. SET and UTCI registered lower values of 12 % and 2 % respectively. In fact, SET shifted from 52.70 °C for P1 to 59.20 °C for P4; conversely, UTCI seems to be less impacted by the different exposition of the points (Fig. 5), moving from 47 °C to 47.20 °C.

Choosing PET, due to its higher value, its maximum reached is 75.8 °C at P9 (LT2), followed by 74.1 °C at P5 (FR). The PET trend comfort index at varying irradiation is shown in Fig. 6 for each exposition and point. As can be seen, their values are higher in the sunny areas (facades LT1 and FR) than those defined in the shaded ones (facades LT2 and FR). In general, the average radiant temperature (T_{mr}), is dependent from the solar radiation, which is one of the main parameters in well-being perception. As the irradiation decreases, the differences between the points are less marked, because of the lower T_{mr}. Moreover, the decrease in irradiation, and a lower exposition to the sun, allows for better a comfort for pedestrians. Since the model is developed for an isolated building, the points exposed to the higher solar radiation (especially in the case with 1400\600 W/m^2) registered higher values. Conversely, its minimum values are in P3 and P2 (LT1), 33.7 °C and 33.9 °C respectively.

3.2. Building's height effect on thermal comfort

To evaluate of PET, SET, and UTCI changes along the façade (LT1), one of the combinations is chosen (H = 5 m, U = 0.5 m/s, RH = 50 %, I = 1000\400 W/m^2). In general, thermal outdoor indexes follow the same trends, obtaining close values at each point (Fig. 7). This underlines that a similar thermal response is reached in the points analysed, although for each indicator this corresponds to a different equivalent temperature.

For convenience, PET has been chosen as reference index as for the irradiation evaluation and in Fig. 8 is showed its behaviour at different building heights. It can be noted that as building's height increases, the

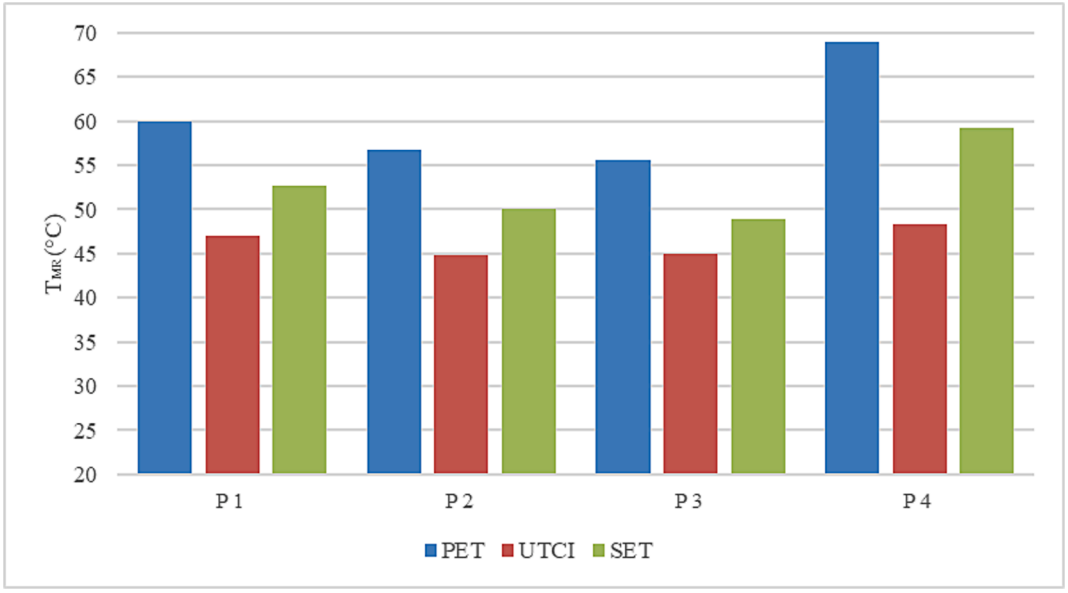

Fig. 5. Results of PET, UTCI e SET obtained for the four points of LT1 surface. The values are calculated at 1000\400 W/m^2 of direct\diffuse solar radiation (W), 10 m of building height (H), 0.50 m/s of wind speed (U) and 0.50 of relative humidity (RH), wherein T_{mr} is the mean radiant temperature in °C.

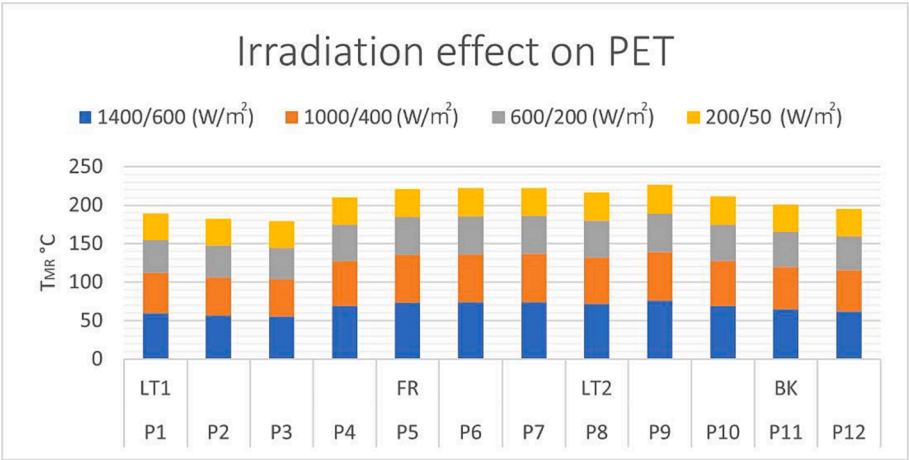

Fig. 6. Cumulative trends of PET as the irradiation varies along LT_1 (a), LT_2 (b), FR (c), BK (d).

comfort of pedestrian increase, as demonstrated in P1, P2 and P3 (LT1). In fact, as example, PET varies from 57,6 °C to 42 °C for P1 when the building height reaches the value of 30 m. Moreover, changing the building height also affects the vortex zone characteristics further increasing thermal comfort [33].

At the sunny points located at LT2 and FR facades, PET values registered a negligible change, >2% (i.e., P5 shift from 62 °C to 61.3 °C). Conversely, P10 showed an increase in terms of comfort, moving from 61.5 to 55.3 °C, due to the contribution of a modified lateral vortex structure [33]. Points located in façade BK are also shaded, therefore, an improvement in outdoor comfort is noticed, especially in points P11 and P12 (10.50 % and 16.70 %, respectively).

3.3. *Wind velocity effect on thermal comfort*

The outdoor thermal comforts have been evaluated at different the wind speed, which vary in a range from 0.1 to 2.0 m/s (Table 2). The first step is to analyse which thermal comfort index is the most influenced, choosing a single combination (I = 1000\400 W/m^2, U = 0.1 m/s, H = 10 m, RH = 50 %). Fig. 8 shows that the two points (P2-P3) within the recirculation area are the most affected, reaching a mean percentage increase of 20 % for each outdoor thermal index. However, in this case, the trend of all indexes is similar. The main change is the equivalent temperature associated with each indicator which is defined by the thermal model adopted.

Based on the curves defined by the three indexes reported in Fig. 9, it is possible to evaluate their evolution around the building by considering only PET as reference indicator as for the other simulations.

Fig. 10 confirms that wind speed increase corresponds to a comfort improvement in the area, due to the decrease of the equivalent temperature perceived by the subject. LT1 represents the most comfortable facades due to the presence of the shadow cone, instead, P3 is the less comfortable, with an improvement of comfort equal to 21 % (from 53.2 °C to 42 °C), followed by P2 with 18 % (53 °C–43.4 °C). Since the points located in the sunny area are very exposed to irradiation, such as FR, they are very sensible to the increase of wind speed. P5 (from 65.6 °C to 53.8 °C) and P6 (from 66 °C to 54 °C) in fact reached an improvement of comfort equal to 18 %. The same assumptions are valid for P8 and P9 in LT2. Conversely, BK faced is less affected by the wind velocity, due to the benefits of the shadow.

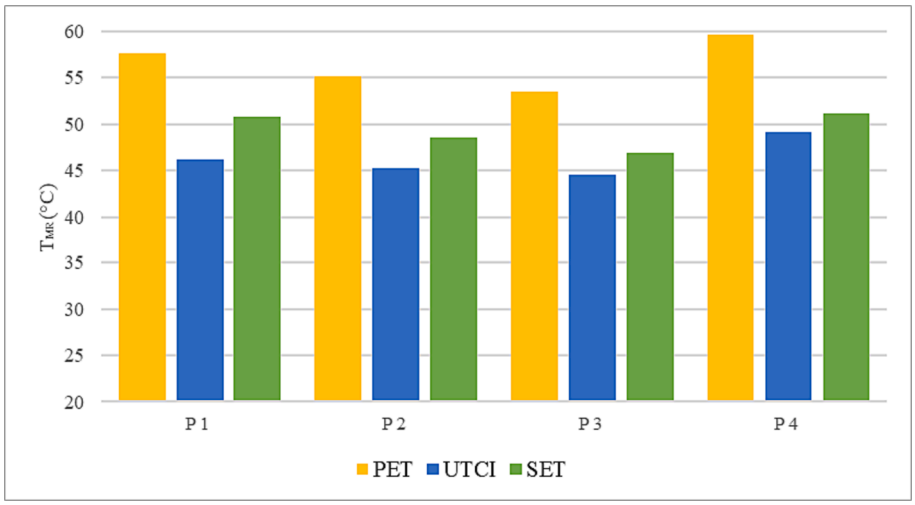

Fig. 7. Trends of PET, UTCI and SET along the LT_1 surface. The values are calculated at 1000\400 W/m^2 of direct\diffuse solar radiation (W), 10 m of building height (H), 0.50 m/s of wind speed (U) and 0.50 of relative humidity (RH).

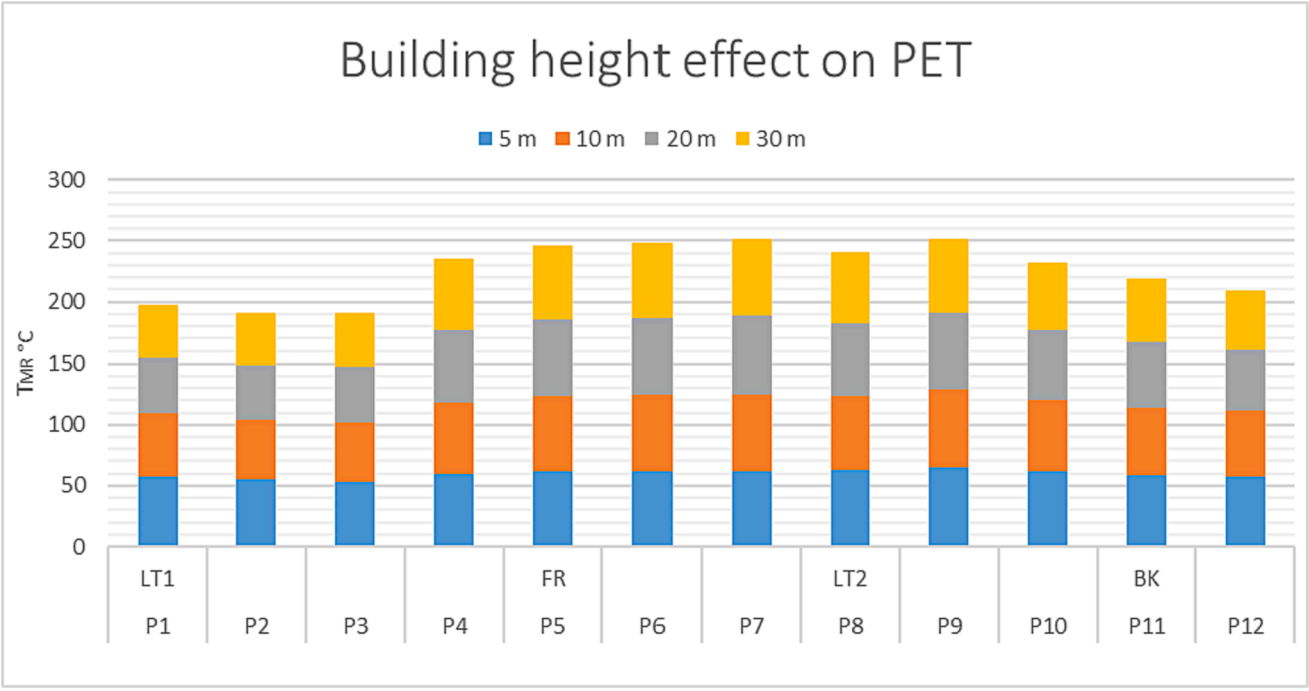

Fig. 8. Impact of building height on the cumulative trends of PET along the facades.

3.4. Relative humidity effect on thermal comfort

The calculation of humidity effect on thermal comfort has been developed keeping fixed the parameters (I = 1000\400 W/m^2, U = 0.5 m/s, H = 10 m and RH = 50 %). The results are showing similar trends as reported in Fig. 11, wherein the maximum percentage difference is below 15 % between points P1 and P4. It must be noted that UTCI index considers the role of humidity in the thermal stress calculation despite of the other models. In fact, the other indicators consider only the body's heat exchange with the atmosphere, where the amount of water in the air plays is considered as negligible.

As reference for showing the variation of thermal comfort UTCI index has been selected. Indeed, PET index is very useful to quantify the impact of the previous variation of parameters (irradiation, building height and velocity), but in this case, it is not suitable due to its independence from the relative humidity value. Therefore, Fig. 12 shows in detail the cumulative variation of UTCI as RH changes (a range from 50 % to 80 %), see Table 2.

In general, both four façades registered a similar trend. Increasing the RH, UTCI values slightly increase around 5–6 % per each point, indifferently from their expositions. As results P1 shifted from 42.7 °C (RH = 50 %) to 45.2 °C (RH = 80 %), providing a decrease of comfort equal to 5.85 %. Therefore, the variation of RH is not so significant, being below 6 %.

3.5. Correlations and discussion

Using the data obtained from the simulation, three different correlations has been developed to predict the outdoor thermal indexes (SET, PET, UTCI). Such correlations are valid inside the rages reported in

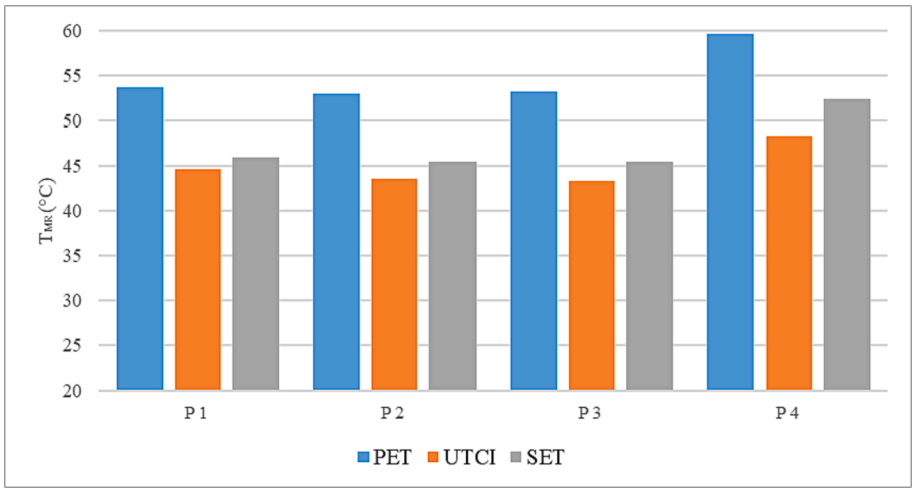

Fig. 9. Trends of PET, UTCI and SET along the surface LT_1. The values are calculated at 1000\400 W/m^2 of direct\diffuse solar radiation (W), 10 m of building height (H), 0.50 m/s of wind speed (U) and 0.50 of relative humidity (RH).

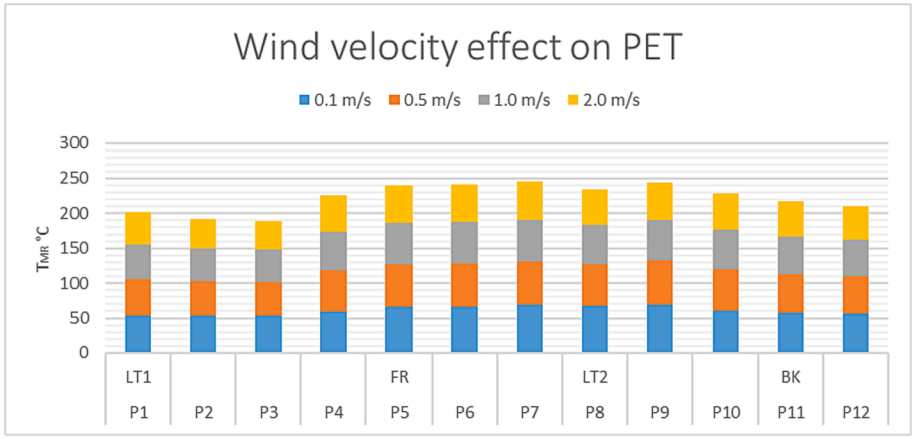

Fig. 10. Cumulative impact of wind velocity on PET along the four façades.

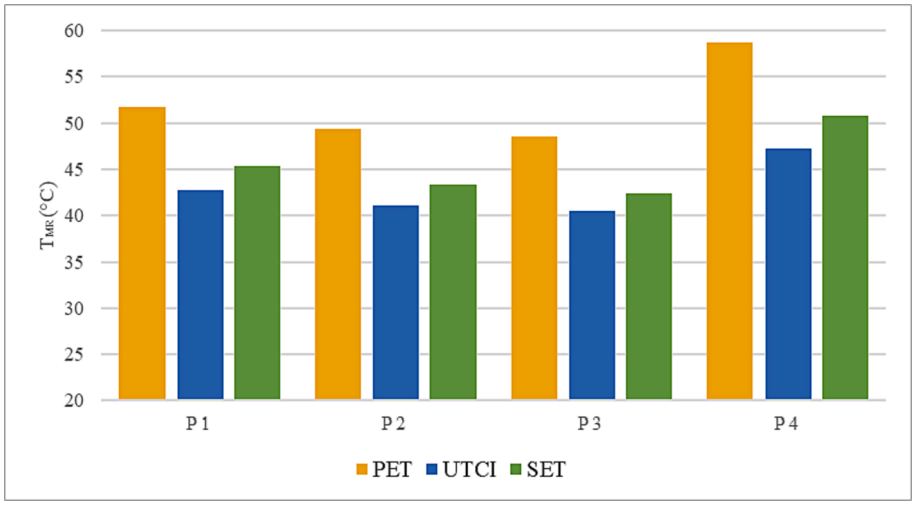

Fig. 11. Trend of PET, UTCI and SET along LT1 surface. The values are calculated at 1000\400 W/m^2 of direct\diffuse solar radiation (W), 10 m of building height (H), 0.50 m/s of wind speed (U) and 0.50 of relative humidity (RH).

Table 3, that comes from the minimum and maximum values utilized during the simulations.

Relative humidity has been not included since, as exposed in paragraph 3.4, it does not have a significant impact on the thermal index's values.

Two quantitative error metrics have been used to validate the cor-

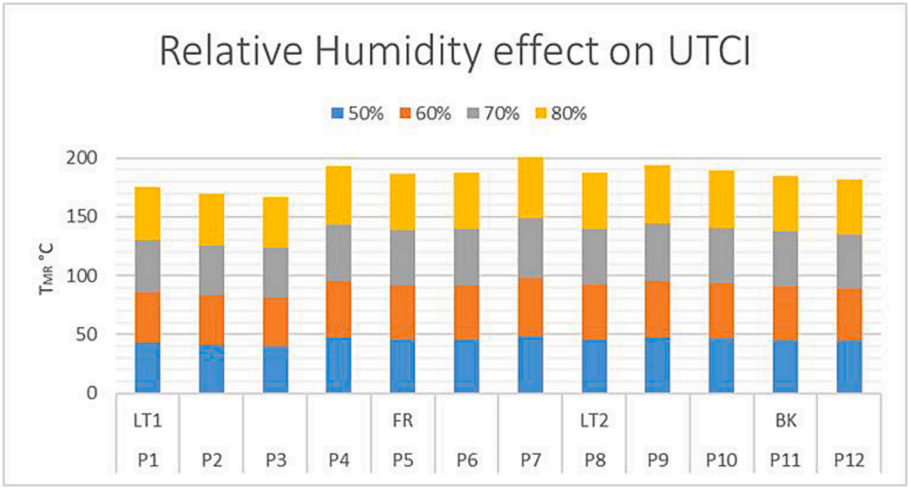

Fig. 12. Cumulative trends of Relative Humidity on UTCI along the four façades.

Table 3
Range values applied to the correlations.

Parameter	Max	Min.
Wind velocity (m/s)	2	0.5
Direct\diffuse irradiation (W/m^2)	1400\600	200\50
Height (m)	30	5
Reynolds number	$4.15{\cdot}10^6$	$3.46{\cdot}10^4$
Stanton number	0.97	0.003
Nusselt number	50170.23	147.03
Prandtl number	0.85	

relation: Root-Mean-Square Error (RMSE) and percentage difference (Δ%). In mathematical terms, the RMSE is an indication of the differences between the values predicted by a model and the values observed. As a result, the RMSE represents accuracy and combines all residuals to form a unique measure of predictability. Instead, percentage difference is a widely diffused metric for model's precision assessment. The formula of RMSE and percentage are expressed in Eqs. (2) and (3).

$$RMSE = \sqrt{\frac{1}{n}\sum_{i=1}^{n}|A_i - F_i|^2} \tag{2}$$

where n iterates over the number of points in the different simulations, A_i is the calculated outdoor thermal comfort (PET; UTCI, SET) with the correlations and F_i is the simulated one.

$$\Delta\% = \left|\frac{(y_1 - y_2)}{y_1} * 100\right| \tag{3}$$

where y_1 refers to the PET value obtained in the simulation and y_2 refers to the PET obtained using the correlation.

The correlations have been calculated for the points P1, P2, P3, P4 on the facade LT_1 using a MATLAB fitting functions. The values used for the correlation development comes from the simulation at the different cases under study. The scope of such correlations is to obtain a simple yet effective tool to develop a quick evaluation of outdoor thermal comfort, avoiding using more complex simulations and metrics to estimate outdoor parameters. Therefore, the correlations used are as simple as possible, avoiding the use of calculated data. In addition, the structure of the correlations follows the others developed by the authors in a previous work [30]. Eq. (1) described the first correlation related to the PET index:

$$f(PET) = (a_1{*}I + b_1) + (c_1 - d_1{*}(H)) + (e_1 - f_1{*}U) \tag{1}$$

where I is the irradiation parameter in [W/m^2], H is the building height in [m] and U is the wind velocity value in [m/s]. The correlations' constants, named a_1, b_1, c_1, d_1, e_1 and f_1, are reported in Table 4.

Table 5 shows the RMSE, and percentage errors obtained using the PET correlation in the twelve cases simulated:

The correlation obtained is composed of three arguments to linearly interpolate the trends of irradiation, the building height and wind velocity. The building height contribution (the second argument) is logarithmic; therefore, it has a different impact on the definition of the PET value. The other two arguments, a and b, are linear (Table 4). Moving to the results, the maximum error value (in bold, Table 5) is obtained by P3 with the corresponding percentage difference of ~3.88 % and a RMSE of ~2.06 points. The total average value of RMSE and Δ% are 0.44 and 0.87 %, respectively, proving the consistency of the correlation obtained. The results have been reported in Fig. 13 for a clear representation understanding of their deviation from the actual vale, Y axis are the simulated values and X axis the correlation's value in the same point.

Moving to UTCI, the developed correlation is reported in Eq. (4). Based on the calculation, the structure of correlation (2) is like Eq. (1) excepting for the constants reported in (Table 6).

$$f(UTCI) = (a_2{*}I + b_2) + (c2 - d_2{*}(H)) + (e_2 - (f_2{*}U)) \tag{4}$$

Table 7 shows the RMSE and percentage errors for the UTCI correlation for the twelve cases simulated.

Also in this case, the impact of building height is predominant, and it is described through a logarithmic trend (Eq. (4)). The highest errors have been registered only for P4, where Δ% is equal to ~4.04 % and RMSE is ~1.65, as pointed out in Table 7 (in bold). Moreover, as for PET, the results have been showed in Fig. 14 where Y axis are the simulated values and X axis the correlation's value in the same point. The total average value of RMSE and percentage difference for UTCI correlation are 0.47 and 1.11 %, respectively.

At least, the correlation of the SET index is reported in Eq. (5) and the relating calculated coefficients are shown in Table 8

$$f(SET) = (a_3{*}I + b_3) + (c_3{*}(H))) + (f_3 - (e_3{*}U)) \tag{5}$$

Table 4
Constants' values used for PET correlation.

	a_1 [°Cm^2/W]	b_1[°C]	c_1[°C/m]	d_1[°C]	e_1 [°Cs/m]	f_1[°C]
P1	0.021	17.29	17.29	8.66	17.29	3.21
P2	0.019	16.62	16.62	7.53	16.62	4.61
P3	0.019	15.07	15.07	5.30	15.07	5.21
P4	0.028	10.94	10.94	0.28	10.94	4.39

Table 5
RMSE and percentage difference values for PET correlation. Maximum errors are reported in bold.

Case	P1		P2		P3		P4	
	|RMSE|	Δ%	|RMSE|	Δ%	|RMSE|	Δ%	|RMSE|	Δ%
1	0.37	0.61	0.64	1.12	0.99	1.77	0.94	1.37
2	0.01	0.02	0.26	0.54	0.55	1.14	0.24	0.41
3	0.04	0.09	0.19	0.46	0.42	1.02	0.03	0.06
4	0.20	0.59	0.22	0.65	0.28	0.84	0.48	1.38
5	0.12	0.20	0.32	0.58	0.78	1.45	0.95	1.58
6	0.01	0.02	0.26	0.54	0.55	1.14	0.24	0.41
7	0.19	0.42	0.15	0.34	0.28	0.62	0.24	0.40
8	0.20	0.46	0.30	0.71	0.67	1.52	0.45	0.77
9	0.60	1.13	1.49	2.81	**2.06**	**3.88**	0.61	1.03
10	0.01	0.02	0.26	0.54	0.55	1.14	0.24	0.41
11	0.11	0.22	0.76	1.63	0.65	1.41	0.26	0.47
12	0.20	0.42	0.65	1.50	0.75	1.82	0.08	0.14
Average value	0.17	0.35	0.46	0.95	0.71	1.48	0.40	0.70

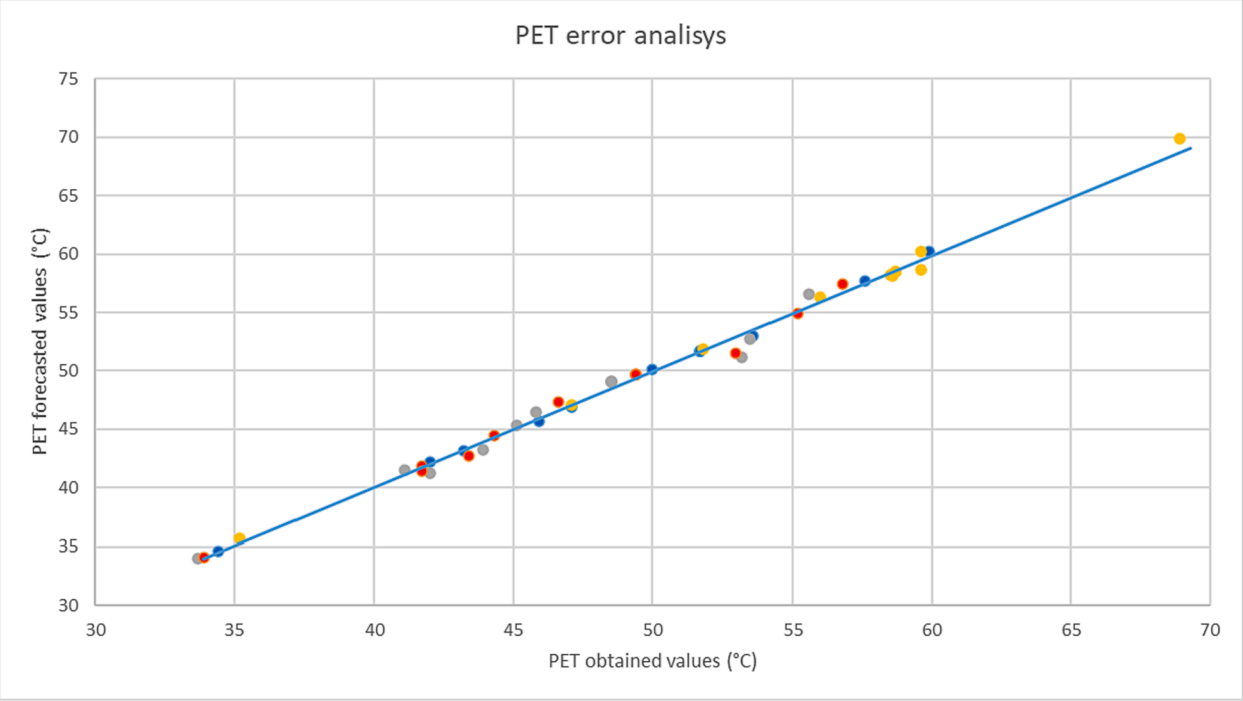

Fig. 13. PET correlation errors.

Table 6
Constants' values used for UTCI correlation. Maximum errors are reported in bold.

	a_2 [°Cm²/w]	b_2[°C]	c_2[°C/m]	d_2[°C]	e_2 [°Cs/m]	f_2[°C]
P1	0.010	13.82	13.82	4.13	13.82	2.01
P2	0.010	13.95	13.95	4.23	13.95	2.69
P3	0.012	13.14	13.14	3.27	13.14	2.96
P4	0.000	17.45	17.45	1.96	17.45	8.94

Table 9 shows the errors obtained using the SET correlation in the twelve cases simulated. The SET correlation has the same structure as the other two showing how a linear interpolation could be used to obtain a good approximation for all the thermal comfort indexes analysed (SET, PET, and UTCI). SET correlation showed the lowest errors if compared to the other two, with a maximum RMSE and Δ% of ~1.47 and ~2.28 % respectively (in bold, Table 9). The results have been showed in Fig. 15 where Y axis are the simulated values and X axis the correlation's value in the same point. The total average value of RMSE and percentage difference are 0.36 and 0,81 %, respectively.

Limitations of this work are regarding the choice of an isolated building, the dimension of the building and the ranges of the physical quantities used in the simulations and reported in Table 3. Future developments will be focused on extending this study to wider models ranges in terms of boundary conditions (i.e., maximum and minimum wind speed, building dimension, temperature, and irradiation) and simulated environment dimension (i.e., up to urban districts). This study follows a previous step developed in the work of [33].

4. Conclusion

As result of climate change, outdoor thermal comfort has become a crucial aspect of sustainable urban development and citizen safety. Despite the positive trend of published papers around the topic, there is still a need of predictive and accurate models for outdoor thermal comfort around a building, able to forecast the outdoor thermal perception of citizens basing on urban and environmental parameters. Scientific community interest has focused mainly on large scale problems, investigating the thermal comfort on large areas such as

Table 7
RMSE and percentage difference values for UTCI correlation.

Case	P1		P2		P3		P4	
	|RMSE|	Δ%	|RMSE|	Δ%	|RMSE|	Δ%	|RMSE|	Δ%
1	0.69	1.49	0.85	1.89	0.40	0.88	0.18	0.37
2	0.19	0.47	0.37	0.91	0.62	1.54	0.18	0.37
3	0.09	0.26	0.20	0.54	0.25	0.68	0.43	0.94
4	0.30	0.91	0.32	0.10	0.07	0.23	0.31	0.70
5	0.43	0.94	0.90	1.98	1.11	2.49	0.82	1.66
6	0.19	0.47	0.37	0.91	0.62	1.54	0.18	0.37
7	0.37	0.91	0.15	0.39	0.04	0.11	0.14	0.30
8	0.04	0.11	0.47	1.25	0.67	1.76	0.43	0.95
9	0.86	1.93	1.05	2.40	0.99	2.30	0.60	1.20
10	0.19	0.47	0.37	0.91	0.62	1.54	0.18	0.37
11	0.35	0.85	0.54	1.33	0.74	1.91	**1.65**	**4.04**
12	0.35	0.85	0.46	1.21	0.51	1.38	0.39	1.15
Average value	0.34	0.80	0.50	1.23	0.56	1.36	0.46	1.04

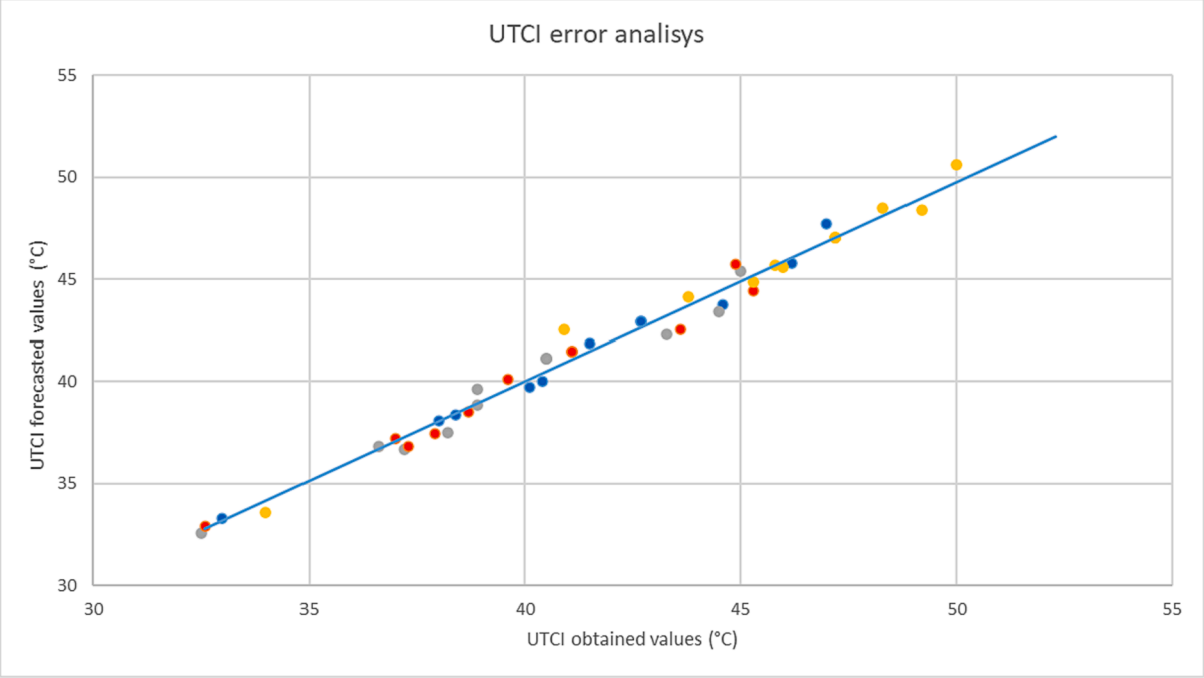

Fig. 14. UTCI correlation errors.

Table 8
Constants' values used for SET correlation. Maximum errors are reported in bold.

	a_3 [°Cm²/w]	b_3[°C]	c_3[°C/m]	d_3[°C]	e_3 [°Cs/m]	f_3[°C]
P1	0.01	14.47	203.49	14.47	16.47	2.88
P2	0.02	13.76	175.72	13.76	15.76	4.09
P3	0.02	12.12	119.79	12.12	14.12	4.65
P4	0.03	8.40	0.04	8.40	10.40	5.20

neighbourhoods, districts, or cities, preferring coverage over adaptability and local accuracy [37], or considering only thermodynamic conditions and not comfort related parameters [34]. The presented study gives a contribution to this topic, filling this gap and analysing the impact of wind velocity, building height, irradiation, and relative humidity on the outdoor thermal comfort indexes (PET, SET and UTCI) near a single building. Three different and simple correlations are proposed to easily calculate thermal comfort indexes. To develop such correlations has been used a coupled model that employs CFD and RayMan/UTCI simulations. As simulation target has been chosen the Mediterranean seasonal average in Rome (303 K) during the day 21 June at 13.00 GMT.

Moving to the results, irradiation seems to be the most significant parameter defining outdoor comfort. As the irradiation decreases, the situation of well-being improves up to 50 % for several points (P5-P9), due to the importance of irradiation in the calculation of the average radiant temperature. The second parameter that affects outdoor thermal comfort is the variation of wind speed, its increase is appreciated by the human body in terms of thermal behaviour. All the points registered an increase of comfort in a range of 14 %–26 %, especially those placed in sunny areas. On the other hand, increasing the height of the building determines a significant improvement in the values only for the points located in a shaded area, up to 26 % (points located in LT1 façade). In fact, direct irradiation is slightly lower in those zones. PET and SET are not influenced by RH, only UTCI shows a slightly negative change according to the RH variation equal to 5 %. As the amount of vapour present in the air increases, at a constant temperature, the body's breathability decreases and therefore the perceived state of discomfort increases.

To develop the correlations a MATLAB fitting functions has been

Table 9
RMSE and percentage difference of SET correlation.

Combination	P1		P2		P3		P4	
	|RMSE|	Δ%	|RMSE|	Δ%	|RMSE|	Δ%	|RMSE|	Δ%
1	0.38	0.72	0.60	1.19	0.88	1.80	**1.47**	**2.28**
2	0.18	0.39	0.00	0.01	0.30	0.70	0.44	0.86
3	0.24	0.63	0.00	0.01	0.21	0.61	0.04	0.11
4	0.31	1.06	0.30	1.05	0.33	1.18	0.75	2.60
5	0.04	0.07	0.33	0.68	0.88	1.88	0.84	1.64
6	0.18	0.39	0.00	0.01	0.30	0.70	0.44	0.86
7	0.32	0.80	0.03	0.07	0.18	0.45	0.14	0.28
8	0.18	0.50	0.22	0.63	0.67	1.75	0.44	0.87
9	0.37	0.81	0.47	1.03	0.94	2.07	0.14	0.28
10	0.18	0.39	0.00	0.01	0.30	0.70	0.44	0.86
11	0.32	0.72	0.35	0.86	0.37	0.93	0.56	1.18
12	0.21	0.51	0.24	0.64	0.38	1.04	0.15	0.35
Average value	0.24	0.58	0.21	0.51	0.48	1.15	0.49	1.01

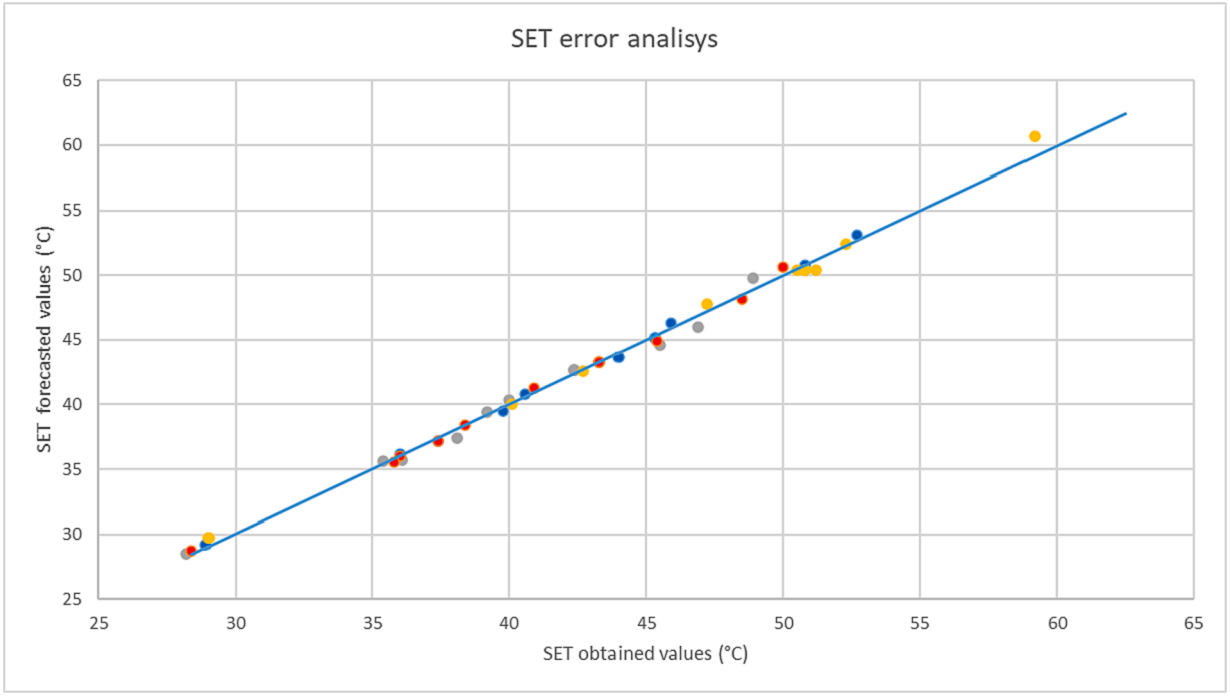

Fig. 15. SET correlation errors.

used for each comfort index varying the solar irradiation, the building height and wind velocity. The relative humidity has been excluded due to its low impact on the overall outdoor thermal comfort indexes. Twelve combinations have been arranged to build the predictive models basing on the simulation results. Then, three different correlations have been proposed for PET, SET and UTCI. PET correlation has a good agreement with the simulated data, showing a mean RMSE and Δ% of ~0.71 and ~1.48 % respectively. Conversely, UTCI correlation reached higher error values, but only for P4, wherein the percentage difference is equal to 4 % with an RMSE of 1.65, wherein the average RMSE and Δ% is attested to ~0.56 and ~1.36 %. Moving to the last comfort index, SET correlation has the lowest errors if compared to the other two, with a mean RMSE and Δ % of ~0.49 and ~1.15 % respectively. As future work, the range for the correlation as well as the interaction with other buildings inside an urban settlement will be studied, expanding the correlation validity ranges. The proposed models can be used independently from location being based on physical CFD simulations. They were developed using as hypotheses data coming from central Europe (Rome) and are validated for similar environmental conditions (Table 2) on isolated buildings. Therefore, the errors can change for conditions far from the simulated and in future will be inspected the possibility to assess their performances also for other climatic areas.

CRediT authorship contribution statement

Laura Pompei: Conceptualization, Data curation, Investigation, Methodology, Software, Visualization, Writing – original draft, Writing – review & editing. **Fabio Nardecchia:** Conceptualization, Data curation, Formal analysis, Methodology, Software, Validation, Writing – original draft, Writing – review & editing. **Luca Gugliermetti:** Data curation, Formal analysis, Investigation, Supervision, Validation, Visualization, Writing – original draft, Writing – review & editing. **Federico Cinquepalmi:** Project administration, Resources, Supervision, Visualization.

Declaration of competing interest

The authors declare that they have no known competing financial interests or personal relationships that could have appeared to influence the work reported in this paper.

Data availability

Data will be made available on request.

Acknowledgement

The present work has been founded by the National Recovery and Resilience Plan (PNNR), Mission 4 Component 2 Investment 1.5 – Call for tender No. 3277of 30/12/2021 of Italian Ministry of University and Research funded by the European Union – NextGenerationEU.

References

[1] M. Saha, A. Al Kafy, A. Bakshi, A. Al Faisal, A.I. Almulhim, Z.A. Rahaman, A. Al Rakib, M.A. Fattah, K.S. Akter, M.T. Rahman, M. Zhang, R. Rathi, Modelling microscale impacts assessment of urban expansion on seasonal surface urban heat island intensity using neural network algorithms, Energ. Build. 275 (2022), https://doi.org/10.1016/j.enbuild.2022.112452.
[2] P. Cohen, O. Potchter, A. Matzarakis, Human thermal perception of Coastal Mediterranean outdoor urban environments, Appl. Geogr. 37 (2013) 1–10, https://doi.org/10.1016/j.apgeog.2012.11.001.
[3] J. Niu, J. Liu, T.c. Lee, Z. Lin, C. Mak, K.T. Tse, B.s. Tang, K.C.S. Kwok, A new method to assess spatial variations of outdoor thermal comfort: Onsite monitoring results and implications for precinct planning, Build. Environ. 91 (2015) 263–270, https://doi.org/10.1016/j.buildenv.2015.02.017.
[4] F. Nardecchia, L. Pompei, F. Bisegna, Environmental parameters assessment of a new diffuser for air cooling/heating system: measurements and numerical validation, Build. Simul. 15 (2022) 1111–1132, https://doi.org/10.1007/s12273-021-0863-y.
[5] T. Xu, R. Yao, C. Du, B. Li, F. Fang, A quantitative evaluation model of outdoor dynamic thermal comfort and adaptation: a year-long longitudinal field study, Build. Environ. 237 (2023), https://doi.org/10.1016/j.buildenv.2023.110308.
[6] J. Li, N. Liu, The perception, optimization strategies and prospects of outdoor thermal comfort in China: a review, Build. Environ. 170 (2020), https://doi.org/10.1016/j.buildenv.2019.106614.
[7] G. Vaishali, R.M.D. Verma, Influence of temperature and relative humidity on PM2.5 concentration over Delhi, Mapan, J. Metrol. Soc. India (2023), https://doi.org/10.1007/s12647-023-00656-8.
[8] P. Azimi, H. Zhao, T. Fazli, D. Zhao, A. Faramarzi, L. Leung, B. Stephens, Pilot study of the vertical variations in outdoor pollutant concentrations and environmental conditions along the height of a tall building, Build. Environ. 138 (2018) 124–134, https://doi.org/10.1016/j.buildenv.2018.04.031.
[9] A.T. Chan, Indoor-outdoor relationships of particulate matter and nitrogen oxides under different outdoor meteorological conditions, 2002.
[10] I.M.I. Ismail, M.I. Rashid, N. Ali, B.A.S. Altaf, M. Munir, Temperature, humidity and outdoor air quality indicators influence COVID-19 spread rate and mortality in major cities of Saudi Arabia, Environ. Res. 204 (2022), https://doi.org/10.1016/j.envres.2021.112071.
[11] J. Lepeule, A.A. Litonjua, A. Gasparrini, P. Koutrakis, D. Sparrow, P.S. Vokonas, J. Schwartz, Lung function association with outdoor temperature and relative humidity and its interaction with air pollution in the elderly, Environ. Res. 165 (2018) 110–117, https://doi.org/10.1016/j.envres.2018.03.039.
[12] ANSI/ASHRAE Addendum a to ANSI/ASHRAE Standard 55-2020, 2021. www.ashrae.org.
[13] M. Migliari, R. Babut, C. De Gaulmyn, L. Chesne, O. Baverel, The Metamatrix of Thermal Comfort: a compendious graphical methodology for appropriate selection of outdoor thermal comfort indices and thermo-physiological models for human-biometeorology research and urban planning, Sustain. Cities Soc. 81 (2022), https://doi.org/10.1016/j.scs.2022.103852.
[14] L. Schibuola, C. Tambani, A monthly performance comparison of green infrastructures enhancing urban outdoor thermal comfort, Energ. Build. 273 (2022), https://doi.org/10.1016/j.enbuild.2022.112368.
[15] O. Potchter, P. Cohen, T.P. Lin, A. Matzarakis, Outdoor human thermal perception in various climates: a comprehensive review of approaches, methods and quantification, Sci. Total Environ. 631–632 (2018) 390–406, https://doi.org/10.1016/j.scitotenv.2018.02.276.
[16] D. Fiala, G. Havenith, P. Bröde, B. Kampmann, G. Jendritzky, UTCI-Fiala multi-node model of human heat transfer and temperature regulation, Int. J. Biometeorol. 56 (2012) 429–441, https://doi.org/10.1007/s00484-011-0424-7.
[17] G. Jendritzky, R. de Dear, G. Havenith, UTCI-Why another thermal index? Int. J. Biometeorol. 56 (2012) 421–428, https://doi.org/10.1007/s00484-011-0513-7.
[18] J. Pickup, R.D. Dear, An Outdoor Thermal Comfort Index (OUT-SET*); 15th ICB ICUC, Macquarie University, Sydney, Australia, 1999.
[19] C.R. de Freitas, E.A. Grigorieva, A comparison and appraisal of a comprehensive range of human thermal climate indices, Int. J. Biometeorol. 61 (2017) 487–512, https://doi.org/10.1007/s00484-016-1228-6.
[20] C. Maftei, C. Buta, Application of thermal discomfort indices for the coastal zone of Black Sea, Dobrogea Region, Ovidius University Annals of Constanta, Ser. Civ. Eng. 19 (2017) 87–100, https://doi.org/10.1515/ouacsce-2017-0008.
[21] Y. Wang, Z. Ni, S. Chen, B. Xia, Microclimate regulation and energy saving potential from different urban green infrastructures in a subtropical city, J. Clean. Prod. 226 (2019) 913–927, https://doi.org/10.1016/j.jclepro.2019.04.114.
[22] P. Kumar, A. Sharma, Study on importance, procedure, and scope of outdoor thermal comfort – a review, Sustain. Cities Soc. 61 (2020), https://doi.org/10.1016/j.scs.2020.102297.
[23] F. Ali-Toudert, H. Mayer, Numerical study on the effects of aspect ratio and orientation of an urban street canyon on outdoor thermal comfort in hot and dry climate, Build. Environ. 41 (2006) 94–108, https://doi.org/10.1016/j.buildenv.2005.01.013.
[24] N. Abdollahzadeh, N. Biloria, Outdoor thermal comfort: analyzing the impact of urban configurations on the thermal performance of street canyons in the humid subtropical climate of Sydney, Front. Arch. Res. 10 (2021) 394–409, https://doi.org/10.1016/j.foar.2020.11.006.
[25] M.A. Bakarman, J.D. Chang, The influence of height/width ratio on urban heat island in hot-arid climates, Proc. Eng. Elsevier Ltd (2015) 101–108, https://doi.org/10.1016/j.proeng.2015.08.408.
[26] B. De, M. Mukherjee, Optimisation of canyon orientation and aspect ratio in warm-humid climate: Case of Rajarhat Newtown, India, Urban Clim. 24 (2018) 887–920, https://doi.org/10.1016/j.uclim.2017.11.003.
[27] R. Shah, R.K. Pandit, M.K. Gaur, Urban physics and outdoor thermal comfort for sustainable street canyons using ANN models for composite climate, Alex. Eng. J. 61 (2022) 10871–10896, https://doi.org/10.1016/j.aej.2022.04.024.
[28] B. Blocken, T. Stathopoulos, J. Carmeliet, CFD simulation of the atmospheric boundary layer: wall function problems, Atmos. Environ. 41 (2007) 238–252, https://doi.org/10.1016/j.atmosenv.2006.08.019.
[29] T. Defraeye, B. Blocken, J. Carmeliet, Convective heat transfer coefficients for exterior building surfaces: existing correlations and CFD modelling, in, Energy Convers. Manag. Elsevier Ltd (2011) 512–522, https://doi.org/10.1016/j.enconman.2010.07.026.
[30] Y. Tominaga, S.i. Akabayashi, T. Kitahara, Y. Arinami, Air flow around isolated gable-roof buildings with different roof pitches: wind tunnel experiments and CFD simulations, Build. Environ. 84 (2015) 204–213, https://doi.org/10.1016/j.buildenv.2014.11.012.
[31] J.I. Perén, T. van Hooff, B.C.C. Leite, B. Blocken, CFD analysis of cross-ventilation of a generic isolated building with asymmetric opening positions: Impact of roof angle and opening location, Build. Environ. 85 (2015) 263–276, https://doi.org/10.1016/j.buildenv.2014.12.007.
[32] F. Nardecchia, F. Gugliermetti, F. Bisegna, How temperature affects the airflow around a single-block isolated building, Energ. Build. 118 (2016) 142–151, https://doi.org/10.1016/j.enbuild.2016.03.003.
[33] F. Nardecchia, B. Mattoni, C. Burattini, F. Bisegna, The impact of humidity on vortex creation around isolated buildings, Build. Res. Inf. 48 (2020) 551–571, https://doi.org/10.1080/09613218.2019.1661762.
[34] R. Aghamolaei, M.M. Azizi, B. Aminzadeh, J. O'Donnell, A comprehensive review of outdoor thermal comfort in urban areas: effective parameters and approaches, Energy Environ. 34 (2023) 2204–2227, https://doi.org/10.1177/0958305X221116176.
[35] Z. Zamani, S. Heidari, P. Hanachi, Reviewing the thermal and microclimatic function of courtyards, Renew. Sustain. Energy Rev. 93 (2018) 580–595, https://doi.org/10.1016/j.rser.2018.05.055.
[36] N. Nasrollahi, M. Hatami, S.R. Khastar, M. Taleghani, Numerical evaluation of thermal comfort in traditional courtyards to develop new microclimate design in a hot and dry climate, Sustain. Cities Soc. 35 (2017) 449–467, https://doi.org/10.1016/j.scs.2017.08.017.
[37] R. Aghamolaei, M. Fallahpour, P.A. Mirzaei, Tempo-spatial thermal comfort analysis of urban heat island with coupling of CFD and building energy simulation, Energ. Build. 251 (2021), https://doi.org/10.1016/j.enbuild.2021.111317.
[38] A. Karimi, A. Bayat, N. Mohammadzadeh, M. Mohajerani, M. Yeganeh, Microclimatic analysis of outdoor thermal comfort of high-rise buildings with different configurations in Tehran: insights from field surveys and thermal comfort indices, Build. Environ. 240 (2023), https://doi.org/10.1016/j.buildenv.2023.110445.
[39] M. Santamouris, R. Paolini, S. Haddad, A. Synnefa, S. Garshasbi, G. Hatvani-Kovacs, K. Gobakis, K. Yenneti, K. Vasilakopoulou, J. Feng, K. Gao, G. Papangelis, A. Dandou, G. Methymaki, P. Portalakis, M. Tombrou, Heat mitigation technologies can improve sustainability in cities. An Holistic Experimental and Numerical Impact Assessment of Urban Overheating and Related Heat Mitigation Strategies on Energy Consumption, Indoor Comfort, Vulnerability and Heat-Related Mortality and Morbidity in Cities, Energ. Build. 217 (2020) 2, https://doi.org/10.1016/j.enbuild.2020.110.
[40] F.R. Menter, R. Lechner, A. German, G.A.M. Nts, S. Petersburg, Best Practice: Generalized k-ω Two-Equation Turbulence Model in ANSYS CFD (GEKO), 2019.
[41] X. Zhang, J.W.G. Buddhika, J. Wang, A.U. Weerasuriya, K.T. Tse, Numerical investigation of effects of trees on cross-ventilation of an isolated building, J. Build. Eng. 73 (2023), https://doi.org/10.1016/j.jobe.2023.106808.
[42] V.C. Tai, J.W. Kai-Seun, P.R. Mathew, L.K. Moey, X. Cheng, D. Baglee, Investigation of varying louver angles and positions on cross ventilation in a generic isolated building using CFD simulation, J. Wind Eng. Ind. Aerodyn. 229 (2022), https://doi.org/10.1016/j.jweia.2022.105172.
[43] Y. Tominaga, A. Mochida, R. Yoshie, H. Kataoka, T. Nozu, M. Yoshikawa, T. Shirasawa, AIJ guidelines for practical applications of CFD to pedestrian wind environment around buildings, J. Wind Eng. Ind. Aerodyn. 96 (2008) 1749–1761, https://doi.org/10.1016/j.jweia.2008.02.058.
[44] B. Launder, D. Spalding, The numerical computation of turbulent flows, Comput. Methods Appl. Mech. Energy 3 (1974) 269–289.
[45] T. Cebeci, P. Bradshaw, Momentum Transfer in Boundary Layers, Hemisphere Publishing, New York, NY, 1977.

[46] S. Bottillo, A. De Lieto Vollaro, G. Galli, A. Vallati, CFD modeling of the impact of solar radiation in a tridimensional urban canyon at different wind conditions, Solar Energy 102 (2014) 212–222, https://doi.org/10.1016/j.solener.2014.01.029.
[47] F. Salata, I. Golasi, R. de Lieto Vollaro, A. de Lieto Vollaro, Outdoor thermal comfort in the Mediterranean area. A transversal study in Rome, Italy, Build. Environ. 96 (2016) 46–61, https://doi.org/10.1016/j.buildenv.2015.11.023.
[48] A. Matzarakis, Modelling of radiation fluxes in urban areas and their relevance to thermal conditions of humans, Third Symposium on the urban environment, American Meteorological Society, pp. 163–164.
[49] A. Matzarakis, F. Rutz, H. Mayer, Modelling radiation fluxes in simple and complex environments – application of the RayMan model, Int. J. Biometeorol. 51 (2007) 323–334, https://doi.org/10.1007/s00484-006-0061-8.
[50] T. Galindo, M.A. Hermida, Effects of thermophysiological and non-thermal factors on outdoor thermal perceptions: the Tomebamba Riverbanks case, Build. Environ. 138 (2018) 235–249, https://doi.org/10.1016/j.buildenv.2018.04.024.